SEPARATION OF DIFFERENT DEFORMATION REGIMES USING PS-INSAR DATA

V.B.H. Ketelaar[(1)] **and R.F. Hanssen**[(1)]

[(1)] *Delft Institute for Earth Observation and Space Technology; Delft University of Technology*
Kluyverweg 1, 2629 HS Delft, The Netherlands
V.B.H.Ketelaar@lr.tudelft.nl; Hanssen@geo.tudelft.nl

ABSTRACT

Interferometric Synthetic Aperture Radar using Permanent Scatterers (PS-InSAR) [2] can be used for analyzing deformation patterns in time and space. 'Permanent Scattering' can be caused by different physical objects in the terrain. As PSs can be physically different, they may describe deformation patterns caused by different phenomena like gas extraction, ground water level variations or foundation instabilities. Separating superposed deformation signals is not trivial. The high precision of the phase data does not automatically lead to a reliable estimation of the deformation parameters. This paper gives a description of possible deformation causes and related scattering characteristics combined with a case study on separating deformation regimes. The results of a PS analysis performed on Rotterdam, the Netherlands, are used. Three classes of deformation mechanisms are discussed in relation with the corresponding scattering properties.

1 INTRODUCTION

The Rotterdam area in the Netherlands contains several gas fields at a few kilometers depth. A number of them have been taken in production by the Nederlandse Aardolie Maatschappij B.V. (NAM). To monitor the subsidence due to gas extraction, the Rotterdam area is periodically leveled by NAM. The expected subsidence in the Rotterdam area varies from 0 to 2 millimeters per year, which is very low.

As leveling is expensive and time consuming the feasibility of using InSAR measurements for monitoring the subsidence due to gas extraction is being investigated. Due to spatial and temporal decorrelation and atmospheric disturbance signal, conventional InSAR is not suitable for this purpose. Therefore a PS analysis has been carried out by TRE/NPA for NAM. For the ascending mode 32 ERS-1/ERS-2 interferograms with a common master have been created in the period 1992-2000. The descending mode dataset consists of 72 interferograms in the period 1992-2002. The resulting PS displacements for each interferogram are defined relative to a presumably stable reference point. As the atmospheric and orbital errors have been estimated during the PS analysis, the PS displacements should be purely caused by deformation along the line of sight.

Since Rotterdam is an urban area, the PS density is relatively high. The extent of the area is 18 by 16 kilometers. For the ascending mode the PS density is 159 PS/km^2 for a coherence threshold of 0.75. For the descending mode this number is 141 PS/km^2, based on a 0.7 coherence threshold. In the deformation regime case study only PSs with coherence higher than 0.9 were used: 22 PS/km^2 for the ascending mode and 12 PS/km^2 for the descending mode.

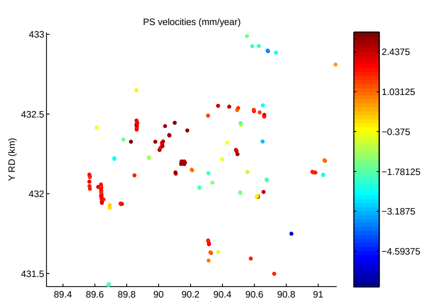

Figure 1: Local variations in PS velocities.

Proc. of FRINGE 2003 Workshop, Frascati, Italy,
1 – 5 December 2003 (ESA SP-550, June 2004) 34_ketelaar

It immediately appeared from the PS displacements that local variations are strong (Fig. 1). The correlation length of the PS displacements is often limited to the building size. PS displacements observed over the same building agree, but PS displacements of a building in the vicinity can have completely different values. As a result, the signal of interest—subsidence due to gas extraction— cannot be estimated directly from the InSAR measurements.

2 PRECISION AND RELIABILITY

An important difference between leveling and InSAR is the physical nature of the measurements. The leveling technique uses well defined points: a bolt in a building or an underground benchmark rigidly fixed to a stable layer. For InSAR it is less clear what the measurements physically represent: does a reflection originate from the roof of a building or is there a multipath effect with the surroundings involved?

InSAR measurements have a high precision, but there is a significant risk that we are not measuring what we want to measure. This problem is related to the 'idealization precision' [3]: how precise does the point we measure represent the displacement we are interested in? This can be generalized to the question how well the actual model applied to the measurements is suited for the estimation of the final parameters of interest. When a longer time series of InSAR data is used, the model parameters can be estimated with a higher precision, but this does not necessarily increase the validity of the used model.

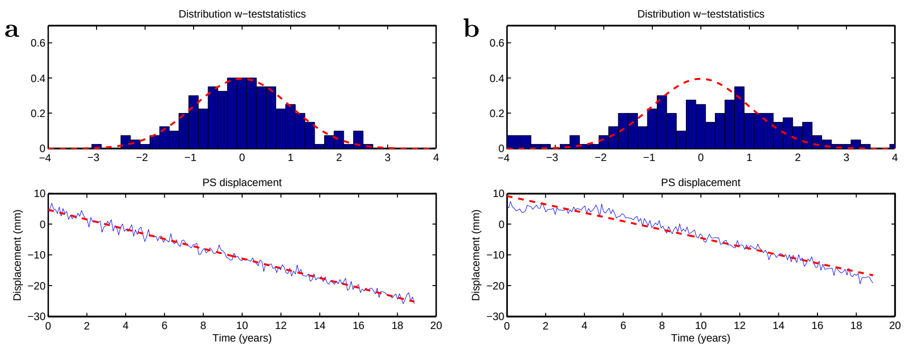

Figure 2: Estimating a linear PS displacement in time: distribution of w-teststatistics.

Fig. 2 shows two simulated PS displacement patterns in time due to gas extraction. In Fig. 2a, the gas production has started before the InSAR time series and the PS is linearly subsiding through the full time span. In Fig. 2b the gas production has started within the InSAR time span, and the PS is starting to subside after a slight delay. This causes a breakpoint in the PS displacement pattern in time. In both situations, a constant velocity has been estimated. As the redundancy in both situations is high, the unknown velocity parameter can be estimated with a high precision. However, looking at the distribution of the w-teststatistics [5] in the second situation, the model discrepancy is visible. It is therefore very important to test the model reliability, both during the PS analysis and the estimation of the deformation parameters. Reliability as defined in geodesy can be split up in internal and external reliability. Internal reliability (minimal detectable bias, MDB) is a measure of the model error that can be detected with a certain probability, whereas the external reliability is defined as the influence of this model error on the estimated unknown parameters. In Fig. 2b the MDB may be small enough to detect the model discrepancy.

3 DEFORMATION CAUSES AND PS TYPE

In the Rotterdam case, subsidence due to gas extraction is contaminated by other spatio-temporal effects: more deformation regimes are present in the same area. As a result, a PS displacement can be a superposition of displacements due to several deformation regimes. Possible deformation regimes are:

- structural instabilities (including foundation),
- shallow mass displacements (ground water level variation and compaction),
- deep mass displacements (gas, oil and mineral extraction).

To be able to relate the movement of a PS to its driving mechanisms it is important to consider the possible scattering characteristics. A PS can be a dominantly single-bounce reflection from a building, but it might as well be a double-bounce reflection (curb-to-wall), comparable to a dihedral corner reflector. This can be extended to multiple bounce effects, for example triple-bounce, comparable to a trihedral corner reflector. Fig. 3 shows possible deformation causes, the difference between a single or double-bounce reflection and deformation detection possibilities. If the physical nature of the PS is unknown, soil compaction can easily be incorrectly interpreted as gas extraction.

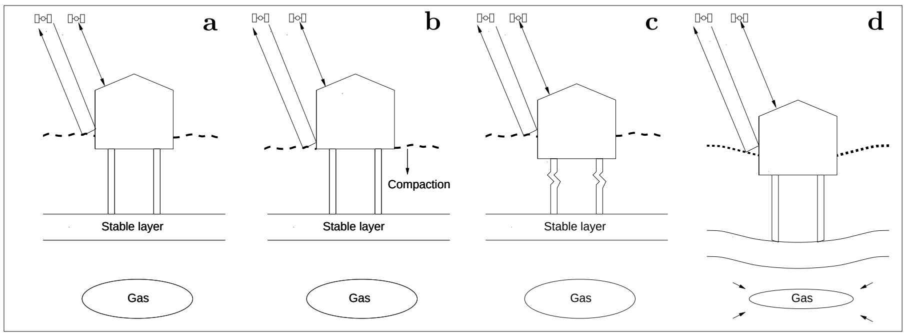

Direct reflection	no change	change	change
Curb-to-wall reflection	change	no change	change

Figure 3: Deformation regimes and their effect on single and double-bounce reflections: (a) reference situation; (b) shallow mass displacement (compaction), affecting only the double-bounce reflection; (c) structural instabilities (foundation), affecting only the single-bounce reflection; (d) deep mass displacement (gas extraction), affecting both the single-bounce and the double-bounce reflection.

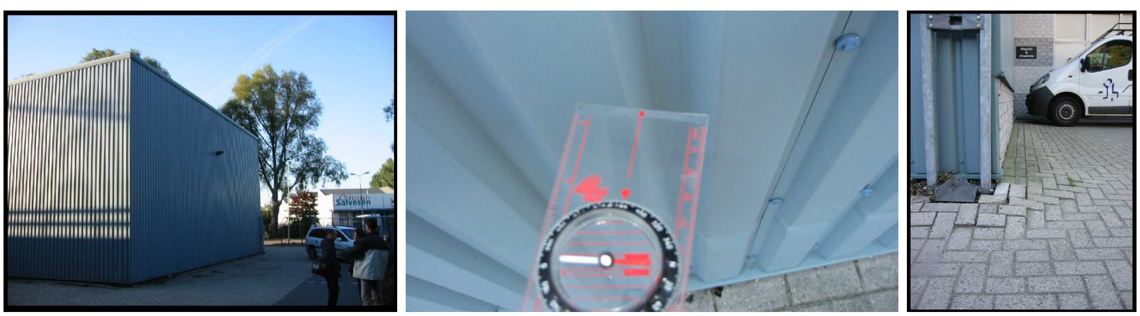

Figure 4: A possible double-bounce curb-to-wall reflection (velocity -9 mm/year).

There are several methods which may benefit the interpretation of the physical representation of a PS. First, polarization may be used to distinguish between even and odd bounced scatterers [6]. In case of odd bounces the phase angle between HH and VV is 180°, for even bounces this is 0°. Unfortunately, no operational satellites have this polarization property currently. A second method is the accurate coregistration of the PS locations with a geographical database. Furthermore InSAR PS heights, which can be determined with a precision of approximately 1.5 meter, might be compared with a 3D city model, to determine whether the dominant reflection stems from the roofs of the buildings or not.

Some of the deformation causes are extremely hard to model. Foundation instabilities can be uncorrelated in space. Compaction depends on the shallow subsurface properties and spatial variation has to be taken into account. It would be preferable to split the movement of a PS up into several deformation components, but if its movement is dominantly due to local effects the PS can be considered as not suitable for monitoring the deformation due to gas extraction.

4 CASE STUDY PS DISPLACEMENTS IN ROTTERDAM

The Rotterdam PS displacements show strong local variations, presumably caused by the superposition of different deformation regimes. Separation of the deformation regime caused of gas extraction has been approached using a purely data-driven and a model-driven method.
The first method is purely data-driven and based on the similarity of the PS displacement pattern in time. For each PS, displacements in millimeters related to a presumably stable reference point for each interferogram are available. Differences between displacement patterns in time between each combination of PSs are calculated as

$$E(k,l) = \sum_{i=t_{start+1}}^{t_{end-1}} (|d_{PS_k}(t_i) - d_{PS_l}(t_i)| \cdot \frac{1}{2}(t_{i+1} - t_{i-1})) \quad (1)$$

where $d_{PS_k}(t_i)$ is the displacement of PS_k from the reference point on time t_i.

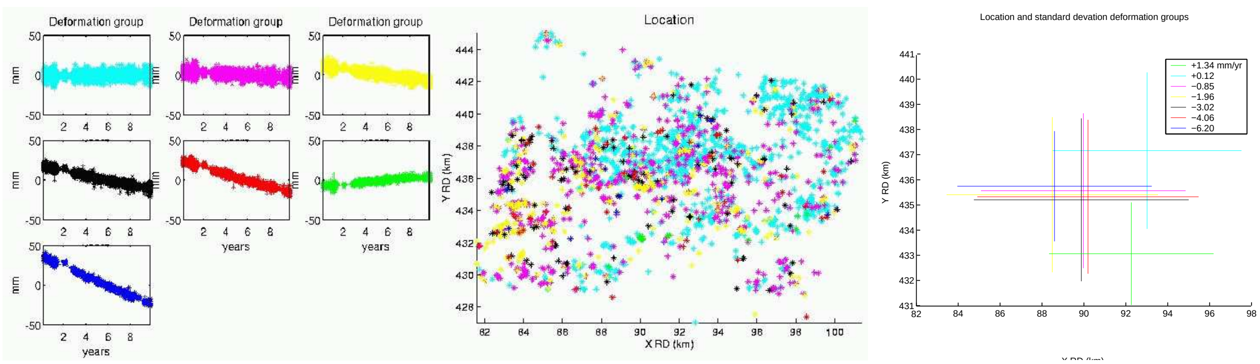

Figure 5: Descending mode: deformation groups.

Fig. 6 shows the division into deformation groups with similar patterns for the descending PSs with coherence higher than 0.9. Looking at the centers of gravity of the locations, deformation groups with a relatively high PS velocity tend to be more concentrated, but their velocity is too high to be caused by gas extraction. The standard deviations in X and Y direction are high for all deformation groups, what means that PSs within a deformation group are distributed over almost the entire area. Intersection with a GIS for the ascending mode revealed that PS within relatively stable regimes have a higher probability to be located on a building. Of course this depends on the idealization of cartographic data and the precision of the PS coordinates.
Separation of deformation groups regarding the displacement pattern can be investigated in a more profound and detailed way, but the main question raised for the displacement patterns is the influence of the choice of estimating a linear or non-linear velocity to a certain degree during the PS analysis itself. Already in this stage the model reliability described in section 2 has to be taken into account.

The second method applied to the Rotterdam PS data uses the prognosis subsidence variogram, based on geological information and reservoir behavior, to select the most suitable PSs for estimating the subsidence due

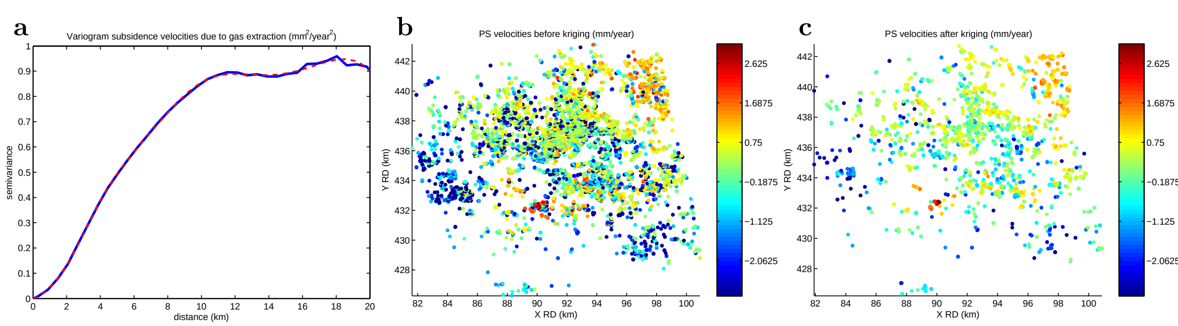

Figure 6: Variogram subsidence prognosis (a) and PS velocities before (b) and after (c) cross-validation.

to gas extraction. Filtering has been applied to the estimated constant velocities of the PSs. For each PS a least squares interpolated (Ordinary Kriging) velocity has been calculated, based on the surrounding velocities using the prognosis variogram to determine the weights [7]. The discrepancy of this interpolated velocity with the actual velocity divided by the measurement and kriging standard deviation forms the cross-validation teststatistic, which is standard normally distributed:

$$Z^*_{OK}(x_0) = \sum_{\alpha=1}^{n} w_\alpha Z(x_\alpha) \qquad T_{PS_\alpha} = \frac{Z(x_\alpha) - Z^*(x_{[\alpha]})}{\sqrt{\sigma^2_{[\alpha]} + \sigma^2_y}} \tag{2}$$

$Z^*_{OK}(x_0)$	Ordinary Kriging value on location x_0, based on n neighbouring points,
w_α	Kriging weight for a neighbouring PS_α based on prognosis semi-variances,
$Z(x_\alpha)$	observed PS_α velocity,
$Z^*(x_{[\alpha]})$	Kriging PS_α velocity, based on n neighbouring points excluding PS_α,
T_{PS_α}	cross-validation teststatistic,
$\sigma_{[\alpha]^2}$	Kriging variance,
σ^2_y	measurement variance.

The Ordinary Kriging estimator is unbiased, as the condition is applied that the sum of the kriging weights should be equal to 1.
The observations used for kriging and cross-validation are the PS velocities. The variance of the velocities has been estimated using the observed displacements in combination with a constant velocity model. In the adjustment and testing sequence the variance component for the observed displacements has been estimated. The results are shown in table 1. As expected the standard deviation of the displacement observations (σ_d) is the same for descending and ascending mode, whereas the precision of the estimated unknown velocity (σ_v) is lower for the descending mode as it contains nearly twice as much observations. Note that the high precision of the velocities does not automatically confirm the reliability of the model.

Table 1: Estimated precision of velocities and displacements, based on a constant velocity model.

	σ_v (mm/yr)	σ_d (mm)
Ascending (32 ifg)	0.12	1.7
Descending (72 ifg)	0.08	1.7

Fig. 6 shows the variogram of the prognosis of the subsidence due to gas extraction in Rotterdam. The semi-variance is approximately 0.8 mm^2/year^2 for a 10 km distance. In Fig. 6c the PS velocities left after cross-validation based on 50 nearest PSs are shown (ascending mode). The subsidence due to gas extraction is now more prominent, but still the local variation remains strong. First attempts to estimate a (high degree) polynomial through the data reveal shortcomings in the chosen model. Because of this and the local variation, the data have not been interpolated, but are directly compared to the prognosis data. Fig. 7b shows that outliers have been successfully eliminated after cross-validation.

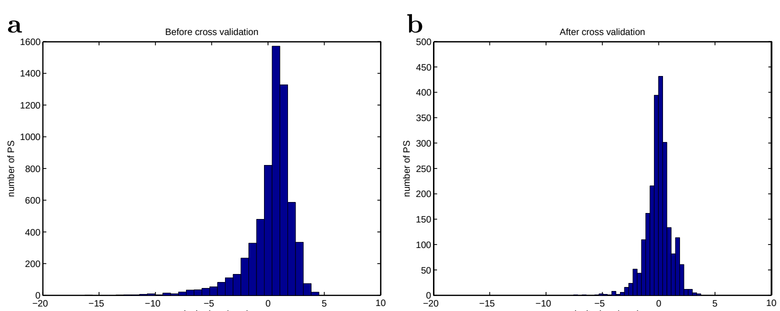

Figure 7: Differences PS velocities - prognosed velocities (mm/year), before (a) and after (b) the cross-validation.

5 CONCLUSIONS

For the Rotterdam area, InSAR observations alone are currently not sufficient for interpreting the possible (geo)physical driving mechanisms of the deformation. Local variations are strong and mask the signal of interest, subsidence due to gas extraction. Knowledge about the physical nature of a PS is indispensable to understand which deformation regimes the displacement of a PS is composed of. Combining this with model imperfections in describing the deformation regimes, leveling data is currently still necessary in Rotterdam. Three deformation mechanisms have been defined that have different responses in the InSAR data, depending on the type of scattering involved. In future research, polarization may be used to distinguish between odd and even bounced reflections. Other possibilities are comparing external city height data with the InSAR heights or using amplitude data.
A data-driven and a model-driven method have been used to separate deformation regimes for the Rotterdam PS data. The model-driven method, based on cross-validation using the subsidence prognosis variogram, reveals a PS velocity pattern more similar to the gas extraction pattern. However, local variations remain strong and it would be preferable not to reject PSs but to split the PS displacement up into deformation components. The fact that the PS data are unevenly distributed limits the applicable methods.
Regarding the modeling of the measurements, the next step is estimating a spatio-temporal model through the PS displacements left after cross-validation and combining this with the leveling data. In [8] a successful application of the trend-signal procedure using both leveling and InSAR data is described. In all stages it is important to guard the model reliability besides the measurement precision.

ACKNOWLEGDEMENTS

This work is part of a PhD research in cooperation with Nederlandse Aardolie Maatschappij B.V. (NAM). The project is supported by Senter, agency of the Dutch Ministry of Economics.

References

[1] A. Ferretti, C. Prati, and F. Rocca, “Nonlinear subsidence rate estimation using permanent scatterers in differential SAR interferometry,” *IEEE Transactions on Geoscience and Remote Sensing*, vol. 38, no. 5, pp. 2202–2212, Sept. 2000.

[2] ——, “Permanent scatterers in SAR interferometry,” *IEEE Transactions on Geoscience and Remote Sensing*, vol. 39, no. 1, pp. 8–20, Jan. 2001.

[3] W. Baarda, “Reliability and precision of networks,” in *VIIth International Course for Engineering Surveys of high precision*, Darmstadt, Germany, Sept. 1976, pp. 1–11.

[4] P. J. G. Teunissen, *Adjustment theory; an introduction*, 1st ed. Delft: Delft University Press, 2000.

[5] ——, *Testing theory; an introduction*, 1st ed. Delft: Delft University Press, 2000.

[6] D. H. Hoekman and M. J. Quinones, “Forest type classification by airborne SAR in the Columbian Amazon,” in *Second Int. Workshop on ”Retrieval of Bio- and Geophysical Parameters from SAR Data for Land Applications” 21-23 Oct.* Noordwijk, The Netherlands: ESTEC, 1998.

[7] H. Wackernagel, *Multivariate Geostatistics*, 2nd ed. Berlin Heidelberg: Springer-Verlag, 1998.

[8] D. Odijk, F. Kenselaar, and R. Hanssen, “Integration of leveling and InSAR data for land subsidence monitoring,” in 11^{th} *FIG International Symposium on Deformation Measurements, Santorini, Greece, 23–28 May, 2003*, 2003, pp. cdrom, p.8. [Online]. Available: http://www.geo.tudelft.nl/fmr/research/insar/dig/bibliography/papers/odijkfig.pdf